AIAA JOURNAL
Vol. 43, No. 12, December 2005

Two-Phase Oxidizing Flow in Volatile Removal Assembly Reactor Under Microgravity Conditions

Boyun Guo*
University of Louisiana at Lafayette, Lafayette, Louisiana 70504
Donald W. Holder†
NASA Marshall Space Flight Center, Huntsville, Alabama 35812
and
John T. Tester‡
Northern Arizona University, Flagstaff, Arizona 86011

Volatile removal assembly (VRA) is a module installed in the International Space Station for removing contaminants (volatile organics) in the wastewater produced by the crew. The VRA contains a slim pack-bed reactor to perform catalyst oxidation of the wastewater at elevated pressure and temperature under microgravity conditions. Optimal design of the reactor requires a thorough understanding about how the reactor performs under microgravity conditions. The efficiency of catalyst oxidation is controlled by catalyst oxidation kinetics and oxygen gas distribution in the reactor. The process involves bubbly flow in porous media with chemical reactions in microgravity environment, which has not been previously studied. We have developed and used a mathematical model in this study to simulate the organics oxidation process in the VRA reactor. We conclude that 1) the remaining oxygen gas in the VRA reactor should decline exponentially with reactor length; 2) the minimum reactor length required to achieve a complete oxygen utilization is directly proportional to bubble size, oxygen density, and bubble velocity, and inversely proportional to rate of oxidation per unit area and bubble sphericity; 3) gravity affects oxygen utilization through changing several parameters including oxygen bubble size; and 4) the example VRA design is very conservative.

Nomenclature

A_c	=	contact area between oxygen and liquid phases, cm^2
a_c	=	contact area per unit length, cm
C_d	=	drag coefficient
C_{ie}	=	concentration of organics i in the effluent, g/cm^3
C_{ii}	=	concentration of organics i in the influent, g/cm^3
D_{oi}	=	molecular diffusivity of organics i, cm^2/s
d	=	bubble diameter, cm
d_m	=	maximum bubble diameter, cm
e	=	2.718
F	=	formation factor defined as tortuosity divided by porosity of pack bed
g	=	gravitational acceleration, cm/s^2
i	=	organics number index
J	=	total flux rate of organics dispersion, $g/cm^2 \cdot s$
J_{Ci}	=	flux rate of organics i as a result of convection, $g/cm^2 \cdot s$
J_{Di}	=	flux rate of organics i as a result of molecular diffusion, $g/cm^2 \cdot s$
L	=	length of the reactor, cm
Mol_{O_2}	=	molar consumption rate of oxygen, $g \cdot mole/cm^2 \cdot s$
M_{i0}	=	amount of organics i injected into the reactor (input mass) during t_w, g
$\dot{M}_{O_2}$	=	oxygen mass flow rate at the point x distance from the reactor inlet, g/s
$\dot{M}_{O_2-0}$	=	oxygen mass flow rate at the reactor inlet, g/s
$\dot{M}_w$	=	water injection mass rate, g/s
m_i	=	number of moles of oxygen utilization for combusting n_i moles of organics i
N_i	=	m_i/n_i, molar number of oxygen utilization for each mole of organics i
N_{We}	=	Weber number
N_{WeC}	=	critical Weber number
n_b	=	number of bubbles
n_i	=	number of moles of organics i
n_o	=	number of organics components
p_i	=	number of moles of CO_2 produced during oxidizing n_i moles of organics i
q_i	=	number of moles of H_2O produced during oxidizing n_i moles of organics i
R_{O_2}	=	remaining oxygen mass fraction
R_{O_2-L}	=	remaining oxygen at the outlet of the reactor, mass fraction
r_b	=	average bubble radius, cm
r_{O_2}	=	rate of oxidation per unit contact area between oxygen and water, $g/cm^2 \cdot s$
r_p	=	average pore radius, cm
t_w	=	residence time of water in the reactor, s
U_{O_2}	=	oxygen utilization, mass fraction
v_b	=	average velocity of bubbles, cm/s
v_{br}	=	velocity of bubbles relative to the liquid phase, cm/s
v_L	=	liquid velocity, cm/s
v_t	=	terminal velocity, cm/s
v_y	=	average water velocity in the y direction, cm/s
W_{mi}	=	molecular weight of organics i, $g/g \cdot mole$
x	=	distance in the reactor axial direction, cm
y	=	distance in the direction perpendicular to catalyst surface, cm
ΔM_i	=	amount of organics i removed in the reaction, g
ΔM_{O_2}	=	oxygen mass consumption potential in the reaction, g

Received 15 July 2004; revision received 7 May 2005; accepted for publication 27 May 2005.

*Chevron Endowed Professor, P.O. Box 44690, Department of Petroleum Engineering; boyun.guo@louisiana.edu.
†Design Team Lead, Mail Code: FD 21, Flight Project Directorate; donald.w.holder@nasa.gov.
‡Associate Professor, P.O. Box 15600, Department of Mechanical Engineering; john.tester@nau.edu.

$\Delta\rho$ = density difference between liquid and gas phases, g/cm^3
ρ_g = gas density, g/cm^3
ρ_L = liquid density, g/cm^3
ρ_{O_2} = density of oxygen gas, g/cm^3
ρ_w = water density, g/cm^3
σ = interfacial tension, dynes/cm
Ψ_b = average sphericity of oxygen bubbles (the ratio of bubble's shortest diameter to longest diameter)

Introduction

VOLATILE removal assembly (VRA) is a subsystem of the closed environment life support system installed in the International Space Station. It is used for removing contaminants (volatile organics) in the wastewater produced by the space station crews. The major contaminants are ethanol, propylene glycol, and formic acid. Table 1 presents a baseline concentration of these contaminants. The VRA contains a slim pack-bed reactor (3.5-cm-diam and four 28-cm-long tubes in series) to perform catalyst oxidation of wastewater at elevated pressure and temperature under microgravity conditions. In the reactor, these contaminants are combusted with oxygen gas (O_2) to form water and carbon dioxide (CO_2) that dissolves in the water stream. Optimal design of the reactor requires a thorough understanding about how the reactor performs under microgravity conditions.

The VRA reactor falls into the category of packed column reactor. Performance of this type of reactors depends on several factors including chemical reaction kinetics, the total contact area of two fluids, and fluid residence time. These factors are affected by the balance between gravitational and capillary forces through fluid distribution in the reactor.

Previous investigations of fluid distribution have focused on experimental studies and computer simulations under 1-*g* gravitational condition. Experimental studies on two-phase distribution in porous media were conducted back in 1930s.[1,2] It was found that higher content of water exists near the inner wall of the container confining the pack beds. This phenomenon is referred to as wall effect. Weekman and Myers[3] studied characteristics of concurrent downward air–water flow in packed beds through laboratory experiments. They found three flow regimes, that is, gas continuous flow, transition or rippling flow, and pulsing flow. Their impact tube measurements confirmed the wall effect. Wilkinson and Wilkinson[4] and Wilknison[5] conducted computer simulations on invasion of water into oil by capillary force in lattices consisting of different types of granular particles. They observed power law behavior of the capillary invasion. Frette et al.[6] conducted experimental studies and computer simulations on slow upward-fluid migration in porous media caused by buoyancy. They verified the power law behavior of the capillary invasion. Frette et al.'s result implies that the content of the nonwetting fluid would approach infinity under zero gravity, which is physically impossible in confined porous media.

An investigation of two-phase flow in porous media under microgravity conditions was reported by Noever and Cronise.[7] The water imbibed into gas bubble lattice in a two-dimensional model was observed under weightless conditions. A microgravity condition was achieved by flying parabolas with the soap froths held vertical for 20–25 s. It was found that in the absence of gravity drainage, froth wicking draws excess fluid onto the bubble lattice. Capillary forces only caused fluid transport: a front moved stably and without fluid fingering along a constant-velocity bubble–water contact line.

NASA tested the performance of a VRA reactor under microgravity and ground conditions in 1999. Again the microgravity was achieved by flying parabolas for 20–25 s. They reported that the oxygen holdup in the reactor in microgravity is within the same range as in 1-*g* gravity (25–34%). However, they did observe the reduction in reactor performance based on influent-effluent analysis (see Model Calibration section in this paper). They concluded that the oxygen distribution in microgravity is not as good as in 1-*g* gravity.

Incorporating wall effect and heat transfer, Guo et al.[8] developed a mathematical model that predicts oxygen holdup in the VRA reactor. This model predicts that oxygen holdup in the VRA reactor increases from 27.5% at 1 *g* to 32.5% at 0.01 *g*. However, Guo et al.'s model does not provide information about oxygen distribution in the reactor such as bubble size.

The objective of this study was to develop a mathematical model to interpret experimental data obtained from normal and microgravity conditions and to predict performance of VRA reactor under microgravity conditions. This model can be used for optimizing designs of VRA reactors for future space exploration.

Mathematical Model

A mathematical model has been developed in this study to simulate the oxidation efficiency of the VRA reactor under various gravity conditions. This section describes the model, model parameters, model calibration, and model prediction.

VRA Reactor Performance Model

The longitudinal distribution of the oxygen mass flow rate in the reactor can be expressed as follows (see Appendix A for derivation):

$$\dot{M}_{O_2} = \dot{M}_{O_2-0} \exp\left(\frac{3 r_{O_2} \Psi_b}{r_b \rho_{O_2} v_b} x\right) \tag{1}$$

Equation (1) implies that oxygen mass flow rate should decline exponentially in the longitudinal direction as a result of the consumption of oxygen in the chemical reactions. The decline rate is proportional to the rate of oxidation per unit area and oxygen bubble sphericity, and inversely proportional to bubble size, in situ oxygen density, and bubble velocity. Obviously, the higher the decline rate, the quicker the oxygen is utilized, the better the reactor performance.

Equation (1) suggests the following expression for the remaining oxygen (R_{O_2}):

$$R_{O_2} = \frac{\dot{M}_{O_2}}{\dot{M}_{O_2-0}} = \exp\left(\frac{3 r_{O_2} \Psi_b}{r_b \rho_{O_2} v_b} x\right) \tag{2}$$

Table 1 Baseline concentration of volatile organics in the wastewater

Organics name	Molecular weight	Liquid molecular diffusivity, cm^2/s	Molar number of oxygen utilization	Influent concentration, mg/liter
Acetaldehyde	44.05	0.00006953	2.5	2.74
Acetone	58.08	0.00005924	4	4.41
1-Butanol	74.1	0.00005924	6	1.5
Ethanol	46.07	0.00006953	2.5	39.2
Ethylene glycol	62.07	0.00005924	2.5	5.51
Formaldehyde	30.03	0.00006953	1	5.89
Formic acid	46.03	0.00006953	0.5	49.9
Methanol	32.04	0.00006953	1.5	7.94
Propylene glycol	76.1	0.00005924	4	35.4
1-Propanol	60.1	0.00005924	4.5	0.45
2-Propanol	60.1	0.00005924	4.5	1.6
Urea	60.06	0.00005924	1.5	3.55

It is customary to use the term oxygen utilization U_{O_2} in evaluation of VRA reactor performance. The expression for U_{O_2} can be theoretically derived based on Eq. (2):

$$U_{O_2} = 1 - R_{O_2-L} = 1 - \exp\left(\frac{3r_{O_2}\Psi_b}{r_b\rho_{O_2}v_b}L\right) \tag{3}$$

This equation can be rearranged to get

$$L = \frac{r_b\rho_{O_2}v_b}{3r_{O_2}\Psi_b}\ln\left(\frac{1}{1-U_{O_2}}\right) \tag{4}$$

which can be used to calculate the minimum reactor length required for achieving a desired degree of oxygen utilization U_{O_2}, for instance, 0.99 (or 99%). Equation (4) indicates that the required minimum reactor length is directly proportional to bubble size, oxygen density, and bubble velocity, and inversely proportional to rate of oxidation per unit area and bubble sphericity.

The oxygen mass consumption potential in the reaction is then expressed as

$$\Delta M_{O_2} = U_{O_2}\dot{M}_{O_2-0}\,t_w \tag{5}$$

The water residence time t_w can be calculated based on water injection rate, reactor size, pack-bed porosity, and oxygen holdup in the reactor.

Based on the stoichiometry during oxidation, the amount of organics i removed in the reaction can be expressed as

$$\Delta M_i = \frac{\Delta M_{O_2}W_{mi}}{32N_i} \tag{6}$$

where $N_i = m_i/n_i$ is defined in the following oxidation reaction:

$$n_i[\text{organics}]_i + m_iO_2 \Rightarrow p_iCO_2 + q_iH_2O \tag{7}$$

For a complete oxidation of 2-propanol (IPA), $N_{IPA} = \frac{9}{2}$ or 4.5.

The amount of organics i injected into the reactor (input mass) with influent during t_w is expressed as

$$M_{i0} = C_{ii}\dot{M}_w t_w/\rho_w \tag{8}$$

If the model-calculated ΔM_i is greater than M_{i0}, organics i is expected to be completely removed. If the model-calculated ΔM_i is less than ΔM_{i0}, the remaining concentration of organics i in the effluent is expected to be

$$C_{ie} = \frac{(M_{i0} - \Delta M_i)\rho_w}{\dot{M}_w t_w} \tag{9}$$

Model Parameters

The oxygen mass flow rate at the reactor inlet $\dot{M}_{O_2-0}$ is a design parameter. The density of oxygen gas ρ_{O_2} can be calculated with gas law for ideal gas under given pressure and temperature. The sphericity of bubble Ψ_b can be affected by reactor geometry and gas holdup in the reactor. Because of a lack of means of estimating its value, we used 0.5 throughout this study. The average flow velocity of oxygen bubbles v_b can be estimated based on oxygen injection rate, reactor cross-sectional area, pack-bed porosity, and oxygen holdup. The oxygen holdup is a function of gravity and is estimated with the mathematical model described by Guo et al.[8]

The rate of oxidation per unit water-oxygen contact area r_{O_2} depends on the total flux rate J at which volatile organics disperse to the catalyst surface. The flux rate of organics i caused by molecular diffusion J_{Di} can be calculated with the following equation[9]:

$$J_{Di} = -\frac{D_{oi}}{F}\frac{dC_i}{dy} \tag{10}$$

where dC_i/dy is the concentration gradient of organics i in the direction perpendicular to the bubble surface. The flux rate of organics i caused by convection J_{Ci} can be calculated by using the Taylor equation[10]:

$$J_{Ci} = -\frac{v_y^2 r_p^2}{48D_{oi}}\frac{dC_i}{dy} \tag{11}$$

The flux rate of organics i is therefore expressed as

$$J_i = -\left(\frac{D_{oi}}{F} + \frac{v_y^2 r_p^2}{48D_{oi}}\right)\frac{dC_i}{dy} \tag{12}$$

Assuming that the organics molecules are oxidized immediately upon reaching the oxygen bubble, the molar consumption rate of oxygen Mol_{O_2} per unit water–oxygen contact area can be estimated by

$$Mol_{O_2} = \sum_{i=1}^{n_o}\frac{N_i J_i}{W_{mi}} \tag{13}$$

The rate of oxidation per unit water–oxygen contact area r_{O_2} can be calculated by $r_{O_2} = 32Mol_{O_2}$.

No mathematical model has been found in the literature that can be used for predicting the size and shape of flowing gas bubbles in the porous media. A mathematical model is available for liquid gas systems[11] in the form of $d_m \approx 4\sqrt{(\sigma/g\Delta\rho)}$. This model indicates that if gravity drops from 1 g to 0.01 g, the bubble size would increase by 10-fold, and if gravity drops to 0 g, the bubble size would increase to infinity. This is physically impossible in confined systems based on the results of previous studies.[8] Therefore, a new mathematical model was developed in this study to estimate the size of gas bubbles in a flowing liquid. Derivation of the model is shown in Appendix B. The resultant equation is

$$N_{WeC} = \frac{\rho_L d_m}{g\sigma}\left[1.1548\sqrt{\frac{gd_m(\rho_L - \rho_g)}{\rho_L C_d}} - v_L\right]^2 \tag{14}$$

If all other parameter values are known, the maximum bubble diameter d_m can be solved numerically from Eq. (14). The critical Weber number was determined to be 979 based on matching the calculated bubble diameter to the data (air bubble size in water) given by Clift et al.[11] The C_d drag coefficient is equal to 0.445 for Reynolds' number between 750 and 3.5×10^5 in gas/liquid systems. However, this value might not applicable to two-phase flow in pack beds because the solid catalyst can exert much higher drag force than liquid phase. By matching the calculated oxygen bubble diameter to the observed oxygen bubble length (10–15 cm) under 1-g conditions, we estimated that the drag coefficient in the VRA reactor to be about $C_d = 3.9$.

Although the values of most model parameters can be estimated theoretically, a few of them still remain unknown. These unknown parameters were used as tuning parameters in model calibration. After the model was tuned, the model was used for prediction.

Model Calibration

Two parameters affecting the rate of oxidation per unit area are the concentration gradient dC_i/dy and convection velocity perpendicular to the oxygen bubbles surface v_y. These two parameters were used as model-tuning parameters. The VRA reactor performance data obtained from ethanol oxidation experimental tests conducted in ground and microgravity conditions were used to calibrate the model. It is expected that a complete oxidation of ethanol should go through the following reaction:

$$2CH_3CH_2OH + 6O_2 \Rightarrow 4CO_2 + 6H_2O \tag{15}$$

Obviously, the reaction suggests that the molar number of oxygen utilization for each mole of ethanol is $\frac{6}{2}$ or 3. However, in the test with ground gravity, the reactor influent contained 144 mg/liter of ethanol and no acetic acid. The reactor effluent contained 91 mg/liter of acetic acid and no ethanol. The microgravity condition was achieved during a KC-135 parabola flight. The reactor influent contained

Table 2 Calculated oxygen utilization with reaction-path possibilities

Possible reaction path	Conversion rate, %	Molar number of oxygen	Oxygen utilization	
			1 *g*	0.01 *g*
1 From ethanol to CO_2 and H_2O	100	3	1	1
2 From ethanol to acetic acid, then	100	0.5		
from acetic acid to CO_2 and H_2O	37	2	0.355	——
3 From ethanol to acetic acid, then	100	0.5		
from acetic acid to CO_2 and H_2O	9	2	——	0.215
4 From ethanol to CO_2 and H_2O	100	2.5	0.839	0.833
5 From ethanol to acetic acid, then	100	0.5		
from acetic acid to CO_2 and H_2O	100	2	0.682	0.678

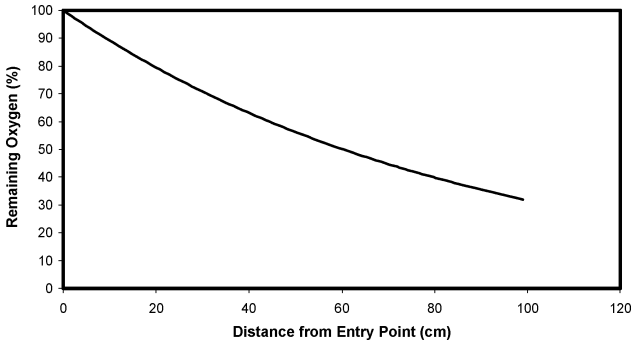

Fig. 1 Calculated remaining oxygen mass profile under 1-*g* conditions for the test reactor.

145 mg/liter of ethanol and no acetic acid. The reactor effluent contained 131.8 mg/liter of acetic acid and no ethanol. Because acetic acid was involved in the tests, the following two-oxidation reactions were anticipated in the reactor:

$$CH_3CH_2OH + O_2 \Rightarrow CH_3COOH + 2H_2O \tag{16}$$

$$CH_3COOH + 2O_2 \Rightarrow 2CO_2 + 2H_2O \tag{17}$$

These two reactions suggest that the molar numbers of oxygen utilization for each mole of ethanol and acetic acid are 1 and 2, respectively. If these two reactions are complete, the overall molar number of oxygen utilization for each mole of ethanol is 3. Therefore, the oxygen utilization is reaction-path dependent. Fast reactions at high temperatures can utilize more oxygen than slow reactions at low temperatures. Table 2 summarizes calculated oxygen utilization with different reaction-path possibilities.

To simulate the VRA reactor that performs complete oxidation reactions at moderate temperature (245°F), the mathematical model [Eq. (3)] was calibrated assuming the fifth reaction path with the molar number of oxygen utilization for each mole of ethanol being 2.5. To achieve the calculated oxygen utilization of 68%, it was assumed that the organics concentrations drop from the initial concentrations at the catalyst surface to zero at the oxygen bubble surfaces within a distance of a half-pore radius. When the convection velocity perpendicular to the oxygen bubble surface was tuned to 0.2766 times the average water velocity in the reactor longitudinal direction, the rate of oxidation per unit area was calculated to be 5.15×10^{-5} g/cm$^2 \cdot$ s. The profile of remaining oxygen calculated with Eq. (2) is presented in Fig. 1. It shows that oxygen mass drops from 100% at the inlet to 32% at the outlet, that is, the oxygen utilized is 68%. Table 3 summarizes other input data used in the mathematical model to compute the performance of the VRA reactor. Some of the data are not required by the mathematical model presented here but are required by the mathematical model described by Guo et al.[8] for oxygen holdup calculations. The density of oxygen gas $\rho_{O_2} = 0.27$ lbm/ft^3 was calculated with gas law using pressure 65 psia and temperature 245°F. Based on Guo et al.'s (2004) mathematical model, oxygen gas holdups were estimated to be 25.5 and 28.5% under 1- and 0.01-*g* conditions. The oxygen and water velocities were calculated to be 0.20 and 0.61 cm/s, respectively, under 1-*g* conditions. They were calculated to be 0.18 and 0.64 cm/s, respectively, under 0.01-*g* conditions.

Table 3 Data used in the reactor performance computations

Parameter	Value
Gravity level	1 and 0.01 *g*
Reactor length	99 cm
Reactor inner radius	1.74 cm
Wall thickness	0.127 cm
Pressure at outlet	65 psia
Temperature at outlet	245°F
Water injection rate	1.89 g/s
Oxygen injection rate	0.000566 g/s
Pack-bed axis angle from gravity	0 deg
Water density	1000 kg/m^3
Oxygen–water contact angle	45 deg
The average pack bed pore radius	0.03 cm
Pack-bed pore tortuosity	1
Pack-bed permeability	264 Darcy
Residual water saturation	0.5
Residual gas saturation	0.15
Water relative permeability coefficient	1
Oxygen relative permeability coefficient	0.023
Water relative permeability index	2.9
Oxygen relative permeability index	2.5
Pack-bed porosity	0.447
Reactor-wall thermal conduction	117 Btu/hr $\cdot$ ft $\cdot$ F
External temperature gradient	0°F/T
Specific heat of fluid	10 kcal/kg $\cdot$ C
External temperature at inlet	250°F
Fluid temperature at inlet	245°F
Oxygen bubble sphericity	0.5
Critical Weber number	979
Drag coefficient	3.9

Model Output

The VRA reactor in the International Space Station is slightly different from the test reactor. The VRA reactor is 112 cm long. Reactor temperature is 265°F, and oxygen injection rate is 0.001 g/s. Wastewater composition is shown in Table 1. Other parameter values are the same as those given in Table 3.

Figure 2 presents calculated oxygen mass flow rate under 1- and 0.01-*g* conditions. In this case, the oxygen utilizations under 1- and 0.01-*g* conditions are 56.29 and 53.05%, respectively. The calculated oxygen utilization drops by 7.4% under microgravity conditions. Table 4 shows the calculated oxidation performance of the VRA reactor. It indicates complete oxidation of all of the contaminants, and the mass consumption potential is much higher than the input mass.

Discussion

Effect of Gravity

Equation (14) gives the maximum bubble diameters of 12.7 and 13.9 cm under 1- and 0.01-*g* conditions, respectively. This means that the maximum bubble diameter should increase by $(r_{b0.01\text{-}g} - r_{b1\text{-}g})/r_{b1\text{-}g} = 9.4\%$ when gravity drops from 1 to 0.01 *g*. Because the oxygen holdups are almost the same under 1 and 0.01 *g*, the number of bubbles should decrease by about $(n_{b1\text{-}g} - n_{b0.01\text{-}g})/n_{b1\text{-}g} = 1 - (r_{1\text{-}g}/r_{0.01\text{-}g})^3 = 23.6\%$ under

Table 4 Calculated oxidation performance of the VRA reactor under 0.01-*g* conditions

Organics name	Input mass, g	Mass consumption potential, g	Effluent concentration, mg/liter
Acetaldehyde	0.00091223	0.0550352098	0
Acetone	0.001468225	0.0453525738	0
1-Butanol	0.000499396	0.0385745057	0
Ethanol	0.013050886	0.0575591537	0
Ethylene glycol	0.001834448	0.0775491882	0
Formaldehyde	0.001960962	0.0937974220	0
Formic acid	0.016613245	0.2875459074	0
Methanol	0.00264347	0.0667170766	0
Propylene glycol	0.011785749	0.0594238588	0
1-Propanol	0.000149819	0.0417146510	0
2-Propanol	0.000532689	0.0417153173	0
Urea	0.001181904	0.1250630894	0

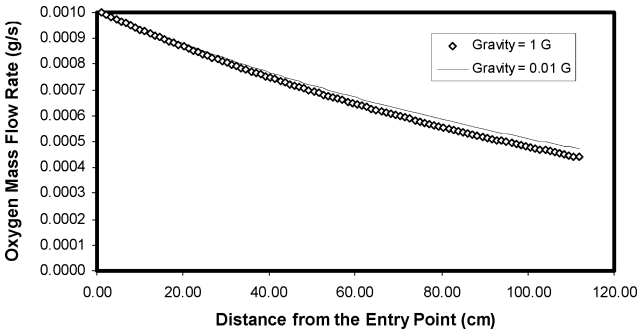

Fig. 2 Calculated oxygen mass flow rate under 1- and 0.01-*g* conditions for the VRA reactor.

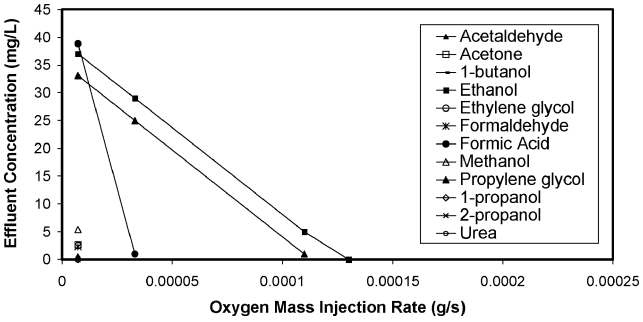

Fig. 3 Calculated effluent concentrations under 0.01-*g* conditions at various oxygen injection rates for the VRA reactor.

0.01-*g* conditions. The total contact area should decrease by $(A_{g1\text{-}g} - A_{g0.01\text{-}g})/A_{g1\text{-}g} = 1 - (r_{1\text{-}g}/r_{0.01\text{-}g}) = 8.6\%$. This means that the oxidation efficiency should decrease by 8.6%.

It appears that a decrease in gravity increases oxygen holdup, which causes oxygen velocity to decrease, and thus theoretically increases overall reaction rate according to Eq. (2). However, the increase in oxygen holdup also causes liquid velocity to increase and thus theoretically increases reaction rate per unit area and speeds up the overall reaction rate. A decrease in gravity increases can also change bubble sphericity, which is more complex to quantify without experimental observation. On the basis of assumed bubble sphericity of 0.5, calculated oxygen utilization drops by 7.4% under microgravity conditions (Fig. 2).

VRA Reactor Performance

To evaluate the oxidation status of the current VRA reactor performance, a sensitivity analysis was performed against oxygen and water injection rates. Figure 3 shows calculated effluent concentrations under 0.01-*g* conditions at reduced oxygen injection rates. It indicates that if the oxygen injection rate drops to 0.00013 g/s,

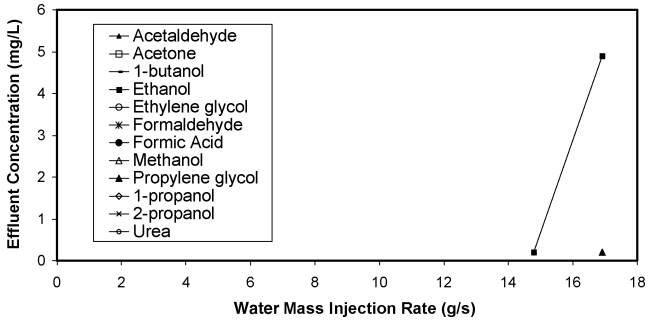

Fig. 4 Calculated effluent concentrations under 0.01-*g* conditions at various water injection rates for the VRA reactor.

ethanol should begin to show up in the effluent. Noticing that the current oxygen injection rate is 0.001 g/s; thus the safety factor is about 0.001/0.00013 or 7.7. If the oxygen injection rate is reduced to 0.00011 g/s, propylene glycol should begin to appear in the effluent. At the oxygen injection rate of 0.000033 g/s, formic acid should appear in the effluent. If the oxygen injection rate is reduced to less than 0.0000072 g/s, almost all of the influent organics should come out in the effluent.

Figure 4 illustrates calculated effluent concentrations under 0.01-*g* conditions at increased water injection rates. It indicates that if the water injection rate increases to 14.79 g/s, ethanol should begin to show up in the effluent. Noticing that the current oxygen injection rate is 1.89 g/s, thus again the safe factor is about 14.79/1.89 or 7.8. If the oxygen injection rate is increased to 16.91 g/s, propylene glycol should begin to appear in the effluent.

Warning: The mathematical model assumes constant concentration of organics in the reactor to calculate dispersion flux rate. This is a safe assumption. Thus the mathematical model should give an overestimate of oxygen utilization.

Conclusions

A mathematical model has been developed in this study to estimate oxidation efficiency in the VRA reactor under microgravity conditions. The following conclusions are drawn:

1) The remaining oxygen gas in the VRA reactor should decline exponentially with reactor length.

2) The minimum reactor length required to achieve complete oxygen utilization is directly proportional to bubble size, oxygen density, and bubble velocity, and inversely proportional to rate of oxidation per unit area and bubble sphericity.

3) Gravity affects oxygen utilization through changing several parameters including oxygen bubble size. More research efforts are required to further investigate the effects of microgravity on VRA reactor performance.

4) The VRA reactor design (defined by the parameters values used in this document) is very conservative. The safety factor is about 7.7.

Appendix A: Derivation of a Mathematical Mode for Oxidation in a Pack-Bed Reactor

Assumptions

The following are four major assumptions made for this modeling effort: 1) concurrent flow of oxygen and water containing small-molecule organics, 2) steady-state bubbly flow regime prevails, 3) geometry and velocity of oxygen bubbles do not change with travel distance, and 4) variations in fluid densities are negligible.

Governing Equation

Figure A1 is a schematic to show oxygen flow rate in a reactor. Suppose an oxygen molecule moves from a point, which is x distance from the reactor entry over a distance Δx during time Δt. Mass balance gives

$$\dot{M}_{O_2-\text{in}} - \dot{M}_{O_2-\text{out}} = \dot{M}_{O_2-c} \tag{A1}$$

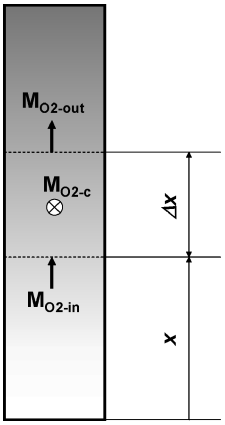

Fig. A1 Schematic to show oxygen flow rate in a vertical reactor.

where $\dot{M}_{O_2-in}$ is the mass flow rate of oxygen at point x, $\dot{M}_{O_2-out}$ is the mass flow rate of oxygen at point $x+\Delta x$, and $\dot{M}_{O_2-c}$ is the mass flow rate of oxygen consumed in chemical reaction in the reactor between the two points. Writing $\dot{M}_{O_2-out} = \dot{M}_{O_2-in} + \Delta\dot{M}_{O_2}$ and

$$\dot{M}_{O_2-c} = r_{O_2} A_c \tag{A2}$$

Eq. (A1) becomes

$$\Delta\dot{M}_{O_2} = -r_{O_2} A_c \tag{A3}$$

The contact area A_c can be assumed to distribute uniformly over the distance Δx, that is, $A_c = a_c \Delta x$. If oxygen bubbles are in spherical shape, a_c can be expressed as

$$a_c = \frac{4\pi r_b^2 n_b}{\Delta x} \tag{A4}$$

Because the volume of a bubble is $V_b = 4\pi r_b^3/3$, Eq. (A4) can be written as

$$a_c = \frac{3 n_b V_b}{r_b \Delta x} \tag{A5}$$

The total volume of bubbles $n_b V_b$ relates to the oxygen mass flow rate $\dot{M}_{O_2}$ and density of oxygen ρ_{O_2} through

$$n_b V_b = \frac{\dot{M}_{O_2} \Delta t}{\rho_{O_2}} \tag{A6}$$

Substituting Eq. (A6) into Eq. (A5) yields

$$a_c = \frac{3\dot{M}_{O_2} \Delta t}{r_b \rho_{O_2} \Delta x} \tag{A7}$$

which, because $\Delta x/\Delta t$ is equal to bubble velocity v_b, becomes

$$a_c = \frac{3\dot{M}_{O_2}}{r_b \rho_{O_2} v_b} \tag{A8}$$

If the oxygen bubbles are not in spherical shape, a sphericity factor Ψ_b defined as the ratio of bubble's shortest diameter to longest diameter can be introduced. Equation (A8) then becomes

$$a_c = \frac{3\Psi_b \dot{M}_{O_2}}{r_b \rho_{O_2} v_b} \tag{A9}$$

Substituting Eq. (A9) into $A_c = a_c \Delta x$ and substituting the latter into Eq. (A3) gives

$$\Delta\dot{M}_{O_2} = -\frac{3 r_{O_2} \Psi_b \dot{M}_{O_2}}{r_b \rho_{O_2} v_b} \Delta x \tag{A10}$$

which, when Δx is an infinitesimal, yields the governing equation of

$$\frac{d\dot{M}_{O_2}}{dx} + \frac{3 r_{O_2} \Psi_b}{r_b \rho_{O_2} v_b} \dot{M}_{O_2} = 0 \tag{A11}$$

Boundary Condition

The boundary condition can be expressed as

$$\dot{M}_{O_2} = \dot{M}_{O_2-0} \qquad \text{at} \qquad x = 0 \tag{A12}$$

where $\dot{M}_{O_2-0}$ is oxygen mass flow rate at reactor entry point.

Solution

Applying boundary condition of Eq. (A12), Eq. (A11) is changed to the integration form of

$$\int_{\dot{M}_{O_2-0}}^{\dot{M}_{O_2}} \frac{d\dot{M}_{O_2}}{\dot{M}_{O_2}} = -\int_0^x \frac{3 r_{O_2} \Psi_b}{r_b \rho_{O_2} v_b} dx \tag{A13}$$

Using the assumption that bubble geometry and velocity do not change with travel distance, Eq. (A13) can be integrated as

$$\dot{M}_{O_2} = \dot{M}_{O_2-0} \exp\left(\frac{3 r_{O_2} \Psi_b}{r_b \rho_{O_2} v_b} x\right) \tag{A14}$$

Appendix B: Derivation of a Mathematical Model for Bubble Size in a Flowing Liquid

Forced rising bubbles in a liquid medium (Fig. B1) are subjected to buoyant force and viscous drag force from the liquid. The drag force has a component F_D from side liquid particles to move the bubble and a component F_d from top liquid particles to resist the motion.

If the liquid is not flowing ($F_D = 0$), the bubble will reach a terminal velocity because of the balance of buoyant force F_b and resistant drag force F_d. This terminal velocity is a function of the size, shape, and density of the bubble and of the density and viscosity of the liquid medium. Force balance gives the following expression for the terminal velocity[11]:

$$v_t = \sqrt{\frac{4gd(\rho_L - \rho_g)}{3\rho_L C_d}} \tag{B1}$$

where $C_d \approx 0.445$ for Reynolds' number between 750 and 3.5×10^5.

If the liquid phase is flowing upward with a velocity v_L, the velocity of bubbles relative to the liquid phase becomes

$$v_{br} = v_t - v_L \tag{B2}$$

Hinze[12] showed that liquid drops moving relative to a gas are subjected to viscous force that tries to shatter the drop, while the interfacial tension acts to hold the drop together. He found that the Weber number, which is defined as the ratio of the inertial force to the interfacial force, controls the dispersion process. Analogous to the liquid drop dispersion process in the continuous gas phase, it is anticipated that the Weber number also controls the bubble dispersion process in the continuous liquid phase in a similar manner. In the latter case, the Weber number N_{We} is defined as

$$N_{We} = \frac{\rho_L v_{br}^2 d}{g\sigma} \tag{B3}$$

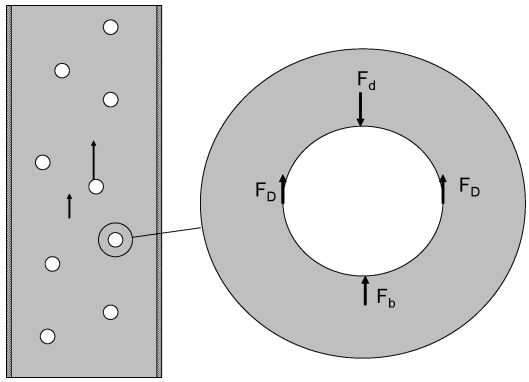

Fig. B1 Forced rising bubbles in a liquid.

where σ is gas-liquid interfacial tension and v_b is bubble velocity. Substituting Eqs. (B1) and (B2) into Eq. (B3) yields

$$N_{\mathrm{We}} = \frac{\rho_L d}{g\sigma}\left[1.1548\sqrt{\frac{gd(\rho_L - \rho_g)}{\rho_L C_d}} - v_L\right]^2 \tag{B4}$$

Hinze[12] showed that if the Weber number exceeded a critical value, a bubble would shatter. If the critical Weber number N_{WeC} is known, Eq. (B4) can be used to compute the maximum bubble diameter d_m, that is,

$$N_{\mathrm{WeC}} = \frac{\rho_L d_m}{g\sigma}\left[1.1548\sqrt{\frac{gd_m(\rho_L - \rho_g)}{\rho_L C_d}} - v_L\right]^2 \tag{B5}$$

Acknowledgments

The authors acknowledge NASA for providing financial support for this research through the NASA Faculty Fellowship Program. The authors are grateful to NASA's Marshall Space Flight Center for its permission to publish technical information.

References

[1]Backer, D. W., Chilton, R. F., and Vernon, D. E., "Distribution of Water in Tower Packing," *Transactions of the American Institute of Chemical Engineering*, Vol. 31, Jan. 1935, pp. 296–299.

[2]Tour, R. S., and Lerman, F., "The Unconfined Distribution of Liquid in Tower Packing," *Transactions of the American Institute of Chemical Engineering*, Vol. 35, April 1939, pp. 719–725.

[3]Weekman, V. W., Jr., and Myers, J. E., "Fluid-Flow Characteristics of Concurrent Gas-Liquid Flow in Packed Beds," *AIChE Journal*, Vol. 10, No. 6, 1964, pp. 951–957.

[4]Wilkinson, D., and Wilkinson, J. F., "Invasion Percolation: A New Form of Percolation Theory," *Journal of Physics A*, Vol. 16, No. 3, 1983, pp. 3365–3370.

[5]Wilkinson, D., "Monte Carlo Study of Invasion Percolation Clusters in Two-Dimensions and Three-Dimensions," *Physics Review A*, Vol. 30, No. 5, 1984, pp. 520–525.

[6]Frette, V., Feder, J., Jossang, T., and Meakin, P., "Buoyancy-Driven Fluid Migration in Porous Media," *Physical Review Letters*, Vol. 68, No. 21, 1992, pp. 3164–3170.

[7]Noever, D. A., and Cronise, R. J., "Weightless Bobble Lattices: A Case of Froth Wicking," *Physics of Fluids*, Vol. 6, No. 7, 1994, pp. 2493–2498.

[8]Guo, B., Holder, D. W., and Layne, C., "Distribution of Flowing Fluids in a Confined Porous Medium Under Microgravity Conditions," *Physics of Fluids*, Vol. 16, No. 8, 2004, pp. 3045–3050.

[9]Lake, L. W., and Hirasaki, G. L., "Taylor's Dispersion in Stratified Porous Media," *Society of Petroleum Engineers Journal*, Vol. 271, Aug. 1981, pp. 459–468.

[10]Taylor, G. I., "Dispersion of Soluble Matter in Solvent Flowing Slowly though a Tube," *Proceedings of the Royal Society of London*, Vol. 219, No. 5, 1953, pp. 186–194.

[11]Clift, R., Grace, J. R., and Weber, M. E., *Bubbles, Drops, and Particles*, Academic Press, New York, 1978, pp. 341–346.

[12]Hinze, J. O., "Fundamentals of the Hydrodynamic Mechanism of Splitting in Dispersion Processes," *AIChE Journal*, Vol. 1, No. 3, 1955, pp. 289–295.

J. Gore
Associate Editor